

Nano-Crystalline $Mg_{(2-x)}Mn_xNi$ Compounds Synthesized by Mechanical Alloying: Microstructure and Electrochemistry

S. Haghighat-Shishavan¹, S. F. Kashani-Bozorg²

Abstract

Mechanical alloying of binary and ternary elemental powder mixtures with the nominal compositions of Mg_2Ni and $Mg_{(2-x)}Mn_xNi$ ($x=0, 0.05, 0.10$ and 0.15 at. %) were carried out in a planetary ball mill for various milling times of 5, 10, 15, 20, 30 and 60 h. X-ray diffraction and field emission scanning and transmission electron microscopy were used for the characterization of the milled products. Clusters of Mg_2Ni -based nano-crystals were produced after 10 h of milling using the binary powder mixture. However, the formation kinetic of Mg_2Ni -based structure was found to increase by increasing Mn content. In addition, Mn was found to decrease Mg_2Ni crystallite size during milling; a mean Mg_2Ni crystallite size of ~ 6 nm was achieved by high energy ball milling of the initial ternary powder mixture of $Mg_{1.85}Mn_{0.15}Ni$ after 60h. The milled product consisted of Mg_2Ni -based crystallites surrounded by amorphous regions. Addition of Mn to Mg_2Ni resulted in increased electrode discharge capacity of the ternary $Mg-Ni-Mn$ milled product compared to that of the binary Mg_2Ni . Moreover, discharge capacity of the milled product was found to increase by increasing milling time. However, this was not followed after 30h of milling possibly due to substantial powder oxidation and formation of $MgNi_2$ phase.

Keywords: Electrochemical properties; High energy ball milling; Mg_2Ni ; Nanocrystalline materials; Mn

1. Introduction

Mg_2Ni -based intermetallic alloy has shown a great potential for the use as hydrogen storage materials recently [1-3]. Melting is the traditional method to produce Mg_2Ni . However, the large differences in the melting point and vapor pressure between the components make difficult the synthesis of a high quality intermetallic. An alternative method for synthesizing Mg_2Ni is the use of mechanical alloying process [4]; this technique was successfully applied to the synthesis of binary nano-crystalline Mg_2Ni using elemental Mg and Ni powders [5]. Nano-crystals often show properties superior to those of conventional materials with coarser structure [6]. Such materials exhibit increased mechanical strength, enhanced diffusivity and other valuable properties as compared to coarse-grained counterparts [7]. Mechanical alloying is a powerful solid-state processing technique to obtain alloys at ambient

temperature and pressure. This technique is commonly used to obtain a high variety of materials including intermetallics, ceramics, solid solutions and metastable phases such as amorphous alloys and supersaturated solutions for hydrogen absorbing applications [8]. The cycle of cold welding and fracturing during mechanical alloying leads to an increase in surface defects and a decrease in crystallite size to the nanometer range [4]. In addition, introduction of third and fourth elements was found to be effective in decreasing Mg_2Ni crystallite size via mechanical alloying [9-10].

The purpose of this work is to synthesize ternary Mg_2Ni -based powder with Mn additives using mechanical alloying and to study the electrochemical properties of the milled products. Influence of partial Mn substitution for Mg was investigated on the structural evolution and microstructures of ternary mechanically alloyed products with

1- Center of Excellence for Surface Engineering and Corrosion Protection of Industries.

2- School of Metallurgy and Materials Engineering, College of Engineering, University of Tehran, Tehran, Iran.

Corresponding author: S. F. Kashani-Bozorg, School of Metallurgy and Materials Engineering, College of Engineering, University of Tehran, Tehran, Iran.

Email: fkashani@ut.ac.ir

stoichiometric compositions of Mg_(2-x)Mn_xNi (x=0, 0.05, 0.10 and 0.15 at.%).

2. Experimental

Elemental powders of Ni (purity 99.00%, ≤10 μm, Merck), Mn (purity 100%, 150 μm, Merck) and Mg flakes (purity 97.80 %, Merck) were mixed and placed into the stainless steel vials (volume 115 ml) according to the stoichiometric compositions of Mg_(2-x)Mn_xNi, (x= 0, 0.05, 0.10, 0.15 at.%). Mechanical alloying was performed by a planetary high-energy ball mill (FP-2 FaraPazhoohesh Isfahan) using hardened chromium steel balls with different diameters under an argon atmosphere in order to protect the powders from environmental attack. A fixed ball to powder weight ratio of 20:1 was used. The milling speed was kept at 600 rpm for periods ranging up to 60 h. The crystal structure of the milled products was investigated by a Philips X'Pert Pro X-ray diffractometer (XRD) using a Cu-K_α radiation (λ=0.15406 nm) and step size of 0.02° over the 2θ range of 10-110°. The crystallite size (d) and lattice strain (ε) were calculated based on X-ray peak broadening using the well-known Williamson-Hall method [4]:

$$\beta = \frac{0.9\lambda}{t(\cos\theta)} + \eta(\tan\theta) \quad (1)$$

where β, t, θ and η are full-width at half maximum height of the peak with maximum intensity (in radian), average crystallite size (in nm), Bragg's angle of the peak and lattice strain, respectively. In this expression using a powder with specified crystallite size, the effect of XRD apparatus on peak broadening was determined and considered in the above formula.

Microstructural evolution during mechanical alloying was observed by means of a field emission scanning electron microscope (FE-SEM).

Electrodes were fabricated by mixing the milled product with nickel powder in a ratio of 1:4. In addition, a small amount of polyvinyl alcohol solution was used as binder to form a paste. The paste was placed on two nickel foam

sheets (150×100 mm) and then mechanically pressed to make a sandwich electrode. Electrochemical measurements of the negative electrode were carried out using a potentiostat/galvanostat, which was interfaced with a computer. The experimental electrodes were tested in a three-electrode open cell, consisting of a metal hydride working electrode, a Ni plate counter electrode and an Hg/HgO reference electrode. In order to reduce the ohmic drop between the working electrode and the reference electrode, the reference electrode was placed close to the working electrode. The electrolyte was a 6 mol/L KOH solution. The negative electrode was initially charged at a constant current of 1000 mA/g for 1 h, after resting for 10 min, it was then discharged at 100 mA/g to a -0.60 V cut-off voltage.

3. Result and Discussion

The XRD patterns of the milled products with initial stoichiometric compositions of Mg_(2-x)Mn_xNi, (x=0, 0.05, 0.10 and 0.15) are shown in Fig.1a to d as a function of milling time. It is clear that the intensity of Mg, Ni and Mn peaks decreases after 5 h of milling. Closer examination of XRD patterns indicates that partial amorphization occurs at early stages of mechanical alloying process. This can be done by a solid state interdiffusion reaction at Mg and Ni boundaries. However, severe mechanical deformation due to mechanical alloying results in a mechanically driven crystallization process. After 10 h of milling, nano-crystals of Mg₂Ni appeared. This crystallization mechanism was first proposed by Ruggeri et al. to explain the formation of nano-crystalline MgNi₂ and Mg₂Ni intermetallic compounds from an amorphous MgNi phase during mechanical alloying [7]. On the other hand, as it can be seen in Figs.1c and d, the Mg₂Ni diffraction peaks appear after 10 h for the case of x=0.1. By increasing the Mn content to x= 0.15, formation kinetic of Mg₂Ni was found to increase; this is probably facilitated by diffusion mechanism caused by increased defect density and rise of temperature during ball milling. Thus, increment of the milling time and Mn content

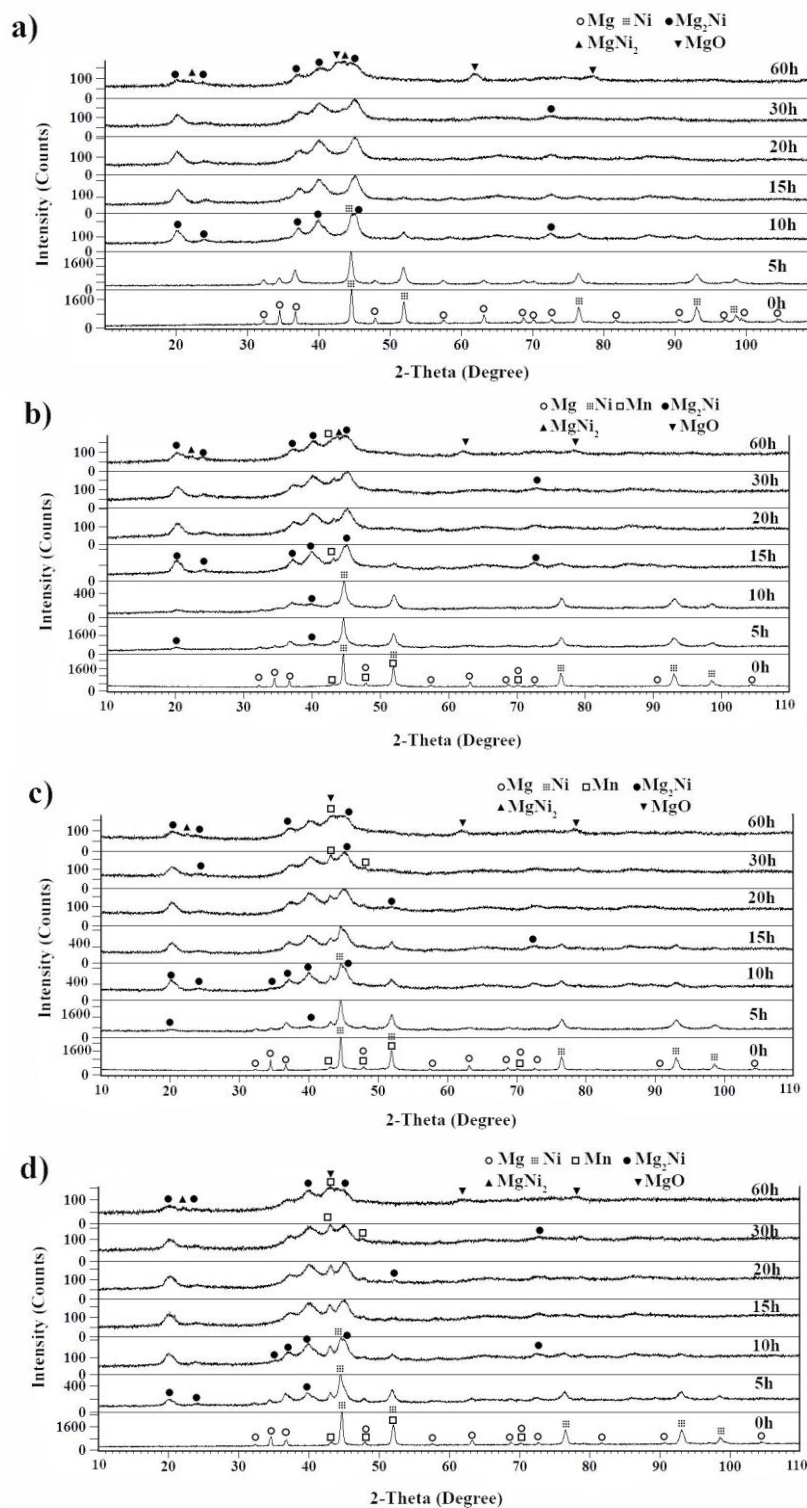


Fig. 1. XRD patterns of the milled products with initial compositions of $Mg_{(2-x)}Mn_xNi$ as a function of milling times: $x=0$ (a), $x=0.05$ (b), $x=0.1$ (c), and $x=0.15$ (d).

are efficient parameters for diminishing the diffraction peaks of Mg and Ni. In the case of binary Mg_2Ni and ternary $Mg_{1.9}Mn_{0.1}Ni$ compounds, Ni diffraction peaks are disappeared after 15 h. However, only 10 h of milling is needed for the vanishing of Ni peaks

in the case of ternary milled product with initial stoichiometric composition of $Mg_{1.85}Mn_{0.15}Ni$.

On the other hand, Mn diffraction peaks still exist after prolonged milling times up to 60 h. This shows that Mn faced difficulties in

substitution for Mg. Such trend was also reported by Huang et al [11-12] on the substitution of Ni by Mn. Since the atomic scattering factor is directly proportional to atomic number of element, the element with lower atomic number has lower atomic scattering factor and intensity and hence with continued milling, diffraction peaks tend to disappear [4]. Here upon, persisting of Mn peaks in XRD patterns may be due to higher atomic number of Mn compared to that of Mg. So, the diffraction peaks of Mn can be observed even after 60 h of milling. There is larger difference in electronegativity between Mg and Ni atoms than those of Mg/Ni with Mn; this is another issue for low solubility of Mn in Ni and Mg crystal structures [12]. Furthermore, from thermodynamic viewpoint, Mg_2Ni is the most stable compound in Mg-Ni binary system, principally due to its negative enthalpy of formation. However, by substitution of Mn for Mg or Ni atoms in Mg_2Ni crystal structure, the stability of ternary Mg_2Ni -based structure decreases because of the less negative enthalpies of formation in comparison with pure binary Mg_2Ni phase. Since the enthalpy of substitution of Mn for Mg is more negative than that of its substitution for Ni [13], the first appearing phase during mechanical alloying whenever Ni substitute by Mn, is Mg_2Ni and it is difficult for Mn to substitute Ni site in Mg_2Ni lattice

structure [12-13]. Therefore, Mn atoms prefer to substitute for Mg sites in Mg_2Ni crystal lattice in comparison with Ni due to most negative enthalpy of formation.

As shown in Figs.1b, c and d, few XRD peaks related to initial elements in powder mixtures overlap with one another. So, when the nano-crystalline Mg_2Ni is formed after 10 h of milling, the interposition of Mg and Ni peaks disappear and two Mn peaks are revealed close to 47.85 and 51.91 degrees. Formation of MgO crystal structure can be identified after 30 h of milling. This is because of opening the milling container in order to scratch the bulk powder sticking to the vial and balls [11]. Gradual broadening of Mg_2Ni peaks occurred as milling time increase from 10 to 60 h; this is principally due to crystallite size reduction and/or micro strain accumulation during mechanical alloying. As Mn has a relatively larger atomic radius than Mg or Ni, addition of Mn to Mg_2Ni alloy, may lead to volume expansion of Mg_2Ni lattice. During mechanical alloying, Mn atoms penetrate into Mg_2Ni crystal and deteriorate long-range order of its lattice; this can promote amorphization process.

Fig.2a and b displays the variations of average crystallite size and lattice strain of Mg_2Ni -based nano-crystals of the milled products using x-ray diffraction results, respectively.

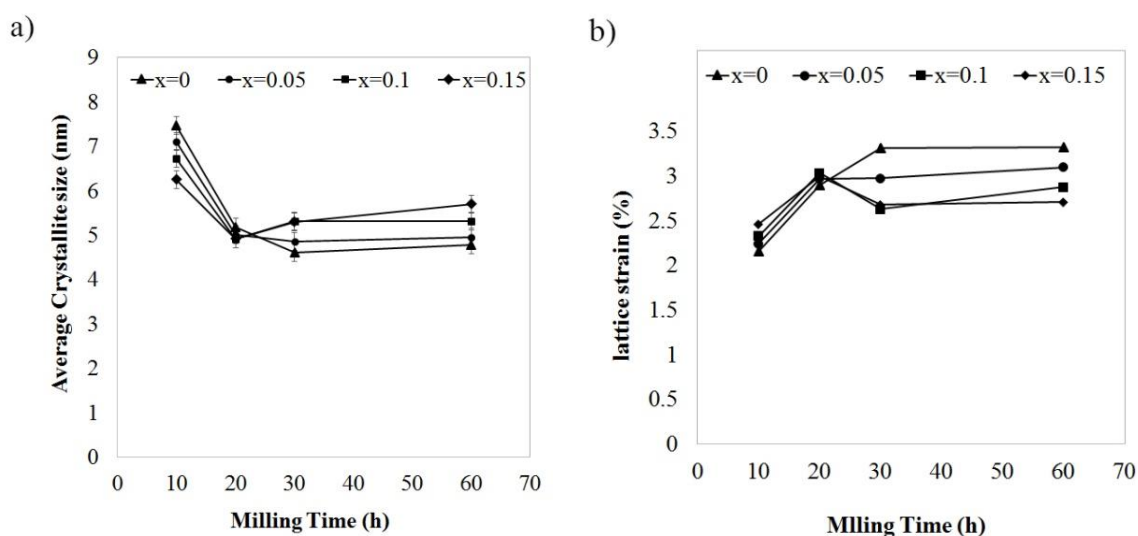


Fig. 2. Variations of average crystallite size (a) and lattice strain (b) of $Mg_{(2-x)}Mn_xNi$ ($x = 0, 0.05, 0.10, 0.15$) compounds as a function of milling times.

As milling time increases, the intensities of Mg_2Ni peaks decrease; these are associated with an increase in lattice strain and decrease in crystallite size. In addition, Fig.2a and b shows that these issues are less pronounced after 20 h of milling since a progressive equilibrium is reached between two processes of mechanical deformation (dislocation generation) and, recovery and recrystallization (elimination or rearrangement of dislocations). Increasing of Mn content leads to an increase in lattice strain and in turn, a decrease in

crystallite size. Mn is naturally more brittle than Mg and Ni. Thus, an increase in Mn content can increase the rate of mechanical deformation which in turn provides crystal refinement and resulting in more easily fracturing [12].

Fig.3 illustrates FE-SEM micrographs of $Mg_{(2-x)}Mn_xNi$, ($x=0, 0.05, 0.10, 0.15$) products after 5 and 60 h of milling.

The morphology of all milled products is characterized by the presence of irregularly-shaped particles with a relatively large size

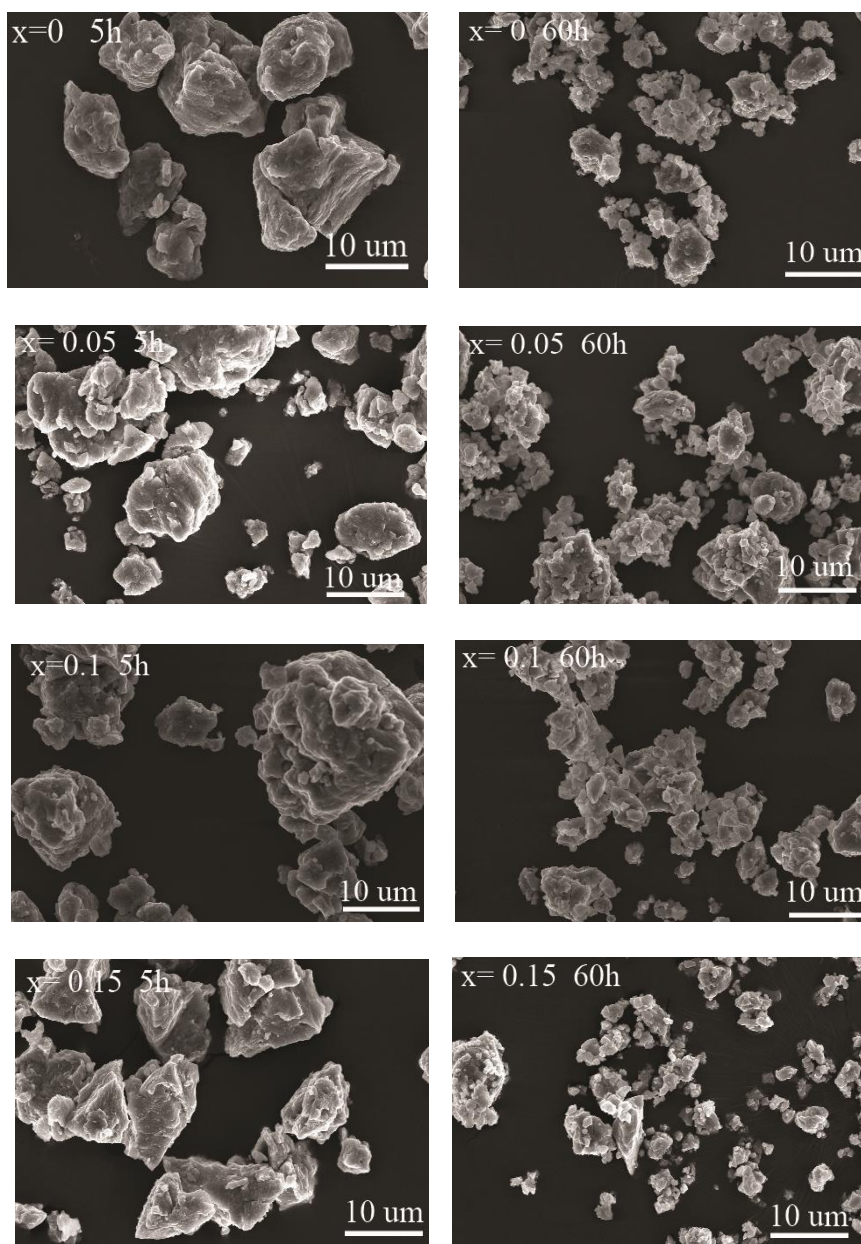


Fig. 3. FE-SEM micrographs of the milled products using initial powder mixtures with stoichiometric composition of $Mg_{(2-x)}Mn_xNi$ ($x= 0, 0.05, 0.1, 0.15$) after 5 and 60 h of milling.

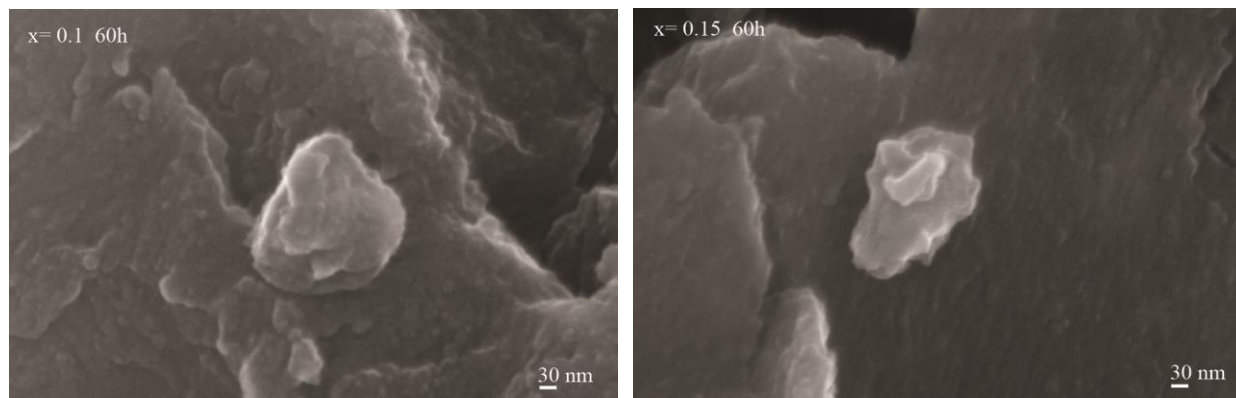


Fig. 4. Higher magnification FE-SEM micrographs of the milled products using initial powder mixtures with stoichiometric composition of $Mg_{(2-x)}Mn_xNi$ ($x = 0.1$, a and 0.15 , b) after 60 h of milling.

distribution, which is in the range of ~ 30 nm to a few microns for the 60h-milled product. In addition, the particle size shows decreasing by increasing Mn content and milling time, a behavior precisely the same as that observed for the crystallite size. Mn powder is relatively brittle. On the other hand due to low solubility of Mn in Ni and Mg crystal structures, fine Mn powders increases the hardness and brittleness of the powder mixtures during milling; this is favorable for the particles to fracture than cold welding [12].

Employing a higher magnification, agglomeration and cold welding of particles were revealed (Fig. 4). It is probable that irregular grain boundaries of nano-crystalline powders encourage particles agglomeration.

Fig. 5a exhibits the milled product to be consisted of accumulation of nano-structured Mg_2Ni -based crystallites. Higher magnification showed small crystallites surrounded by featureless regions (Fig. 5b). The former is the characteristic of amorphous regions. Substantial formation of amorphous regions was confirmed by selected area diffraction pattern analysis that showed a wide diffuse halo (electron diffraction pattern of Fig. 5b); this was in agreement with the observation of hump in X-ray diffraction patterns. In addition, crystallite-size calculations based on X-ray diffraction patterns were found to be consistent with transmission electron microscopy investigations.

As shown in Fig. 6a, the discharge capacity of the fabricated electrodes was found to increase by increasing the amount of Mn from

$x=0$ to $x=0.15$. In addition, the discharge capacity shows increasing by increasing milling time (Fig. 6b). However, 60h-milled product exhibits slight decrease in discharge capacity (Fig. 6b); this can be attributed to the formation of $MgNi_2$ and MgO phases after 60h of milling (Fig. 1d) and their inability to produce hydride.

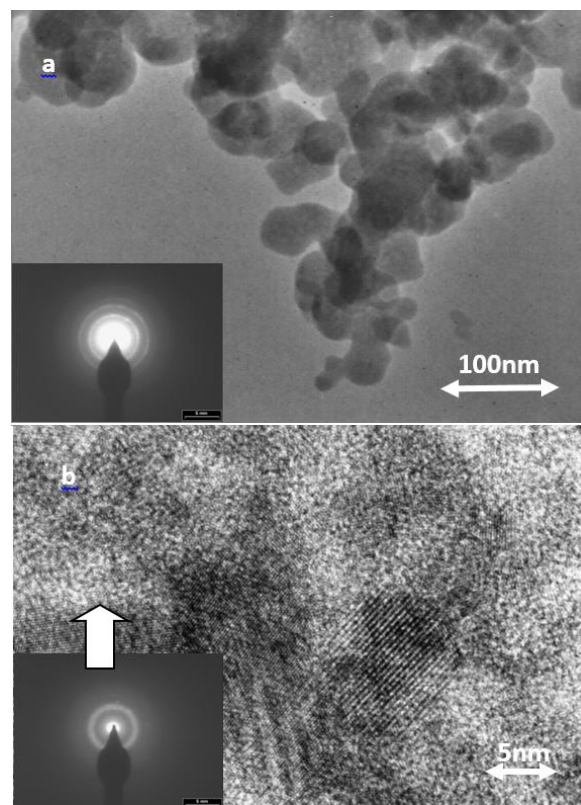


Fig. 5. High resolution transmission electron microscopy of the 60h-milled product with stoichiometric composition of $Mg_{1.85}Mn_{0.15}Ni$; bright field images with their associated electron diffraction patterns showing accumulation of nano-structured Mg_2Ni crystallites (a), and crystallites surrounded by amorphous regions (b).

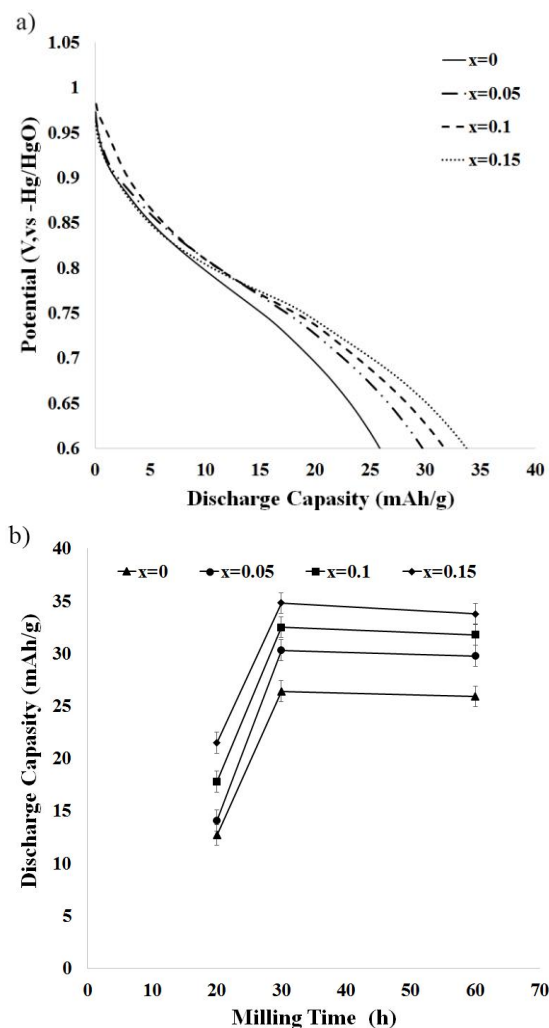


Fig. 5. Electrode properties of $Mg_{(2-x)}Mn_xNi$ ($x=0, 0.05, 0.1, 0.15$ %at)-based compounds; potential vs. discharge capacity (a) and discharge capacity as a function of milling time (b).

4. Conclusions

In summary, effects of Mn addition on the formation and electrochemical properties of Mg_2Ni crystal structure via mechanical alloying were investigated. It was found that increasing of Mn content facilitates the kinetic formation of nano-crystalline Mg_2Ni -based structure. In addition, its crystallite size and lattice strain decreases and increases, respectively. The discharge capacity of the fabricated electrodes from the milled products was found to increase with Mn content.

A maximum discharge capacity of ~ 35 mA/h was measured. On the other hand, this trend was not followed in the case of milling products produced at long milling times (30h and higher); this was attributed to the formation of oxide and $MgNi_2$ phases in the milled products.

Acknowledgment

Partial financial support by Center of Excellence for Surface Engineering and Corrosion Protection of Industries, University of Tehran and Iran Nanotechnology Initiative Council are gratefully acknowledged. Thanks goes to Mr. Masoud Nazarian-Samani for helpful suggestion on high energy ball milling.

References

1. Mohri, M., Kashani-Bozorg, S. F., *J. of Mat. Phys* Vol. 22 (2008) pp.2939-46.
2. Kashani-Bozorg, S. F., Mousavi, S. A., *Nanoscience and Nanotech.*, AIP Vo. 1136 (2009) pp. 710-14.
3. Mohri, M., Kashani-Bozorg, S. F., *Int. J. of Nanosci.* Vol. 10 (2011) pp. 1067-71.
4. Suryanarayana, C, *Prog. Mater. Sci.* Vol. 46 (2001) pp.1-184.
5. Ebrahimi-Purkani, A., Kashani-Bozorg, S. F., *J. Alloys Compd.* Vol. 456 (2008) pp.211-15.
6. Cao, P., Lu, L., Lai, M. O., *Mater. Res. Bull.* Vol. 36 (2001) pp.981-88.
7. Ruggeri, S., Lenain, C., Roue, L., Liang, G., Huot, J., Schulz, R., *J. Alloys Compd.* Vol. 339 (2002) pp.195-201.
8. Gennari, F. C., Esquivel, M. R., *J. Alloys Compd.* Vol. 459 (2008) pp.425-32.
9. Kashani-Bozorg, S. F., Mohri, M., Ebrahimi-Purkani, A, *Adv. Mat. Res.* Vol. 55-57 (2008) pp.581-84.
10. Sharbati M., Kashani-Bozorg, S. F., *Acta Physica Polonica A.* Vol. 121 (2012) pp.211-13.
11. Huang, L. W., Elkedim, O., Jarzebski, M., Hamzaoui, R., Jurczyk, M., *Int. J. Hydrogen Energy* Vol. 35 (2010) pp.6794-6803.
12. Huang, L. W., Elkedim, O., Moutarlier, V., *J. Alloys Compd.* Vol. 504S (2010) pp. 311-314.
13. Huang, L. W., Elkedim, O., Hamzaoui, R., *J. Alloys Compd.* Vol. 509S (2011) pp. 328-333.